Influence of the Phase Morphology on the Molecular Orientation at the Crack Tips in Rubber-Modified Nylon 6: A Micro Fourier Transform Infrared Study

Wenfei Xu, Ruihua Lv, Bing Na, Nana Tian, Zhujun Li

Department of Materials Science and Engineering, East China Institute of Technology, Fuzhou, 344000, People's Republic of China

Received 12 October 2009; accepted 16 January 2010
DOI 10.1002/app.32100
Published online 3 May 2010 in Wiley InterScience (www.interscience.wiley.com).

ABSTRACT: Despite extensive efforts to understand the toughening mechanism of rubber-modified semicrystalline polymers, the plastic deformation event at the crack tips with an extreme deformation gradient and its correlation with phase morphology is, thus far, poorly understood. In this study, micro Fourier transform infrared measurements were adopted to give direct evidence of plastic deformation at the crack tips by the molecular orientation in nylon 6/ethylene–propylene–diene terpolymer (EPDM) blends with a distinct phase morphology. Significant plastic deformation ahead of the crack tips, manifested by a high molecular orientation, was observed in the compatibilized nylon 6/EPDM blends with fine rubber particles. Moreover, the increased transverse crack-propagation resistance due to high molecular orientation dramatically extended the plastic deformation into adjacent regions around the crack tips; this was responsible for enhanced energy dissipation during the fracture process. © 2010 Wiley Periodicals, Inc. J Appl Polym Sci 117: 3139–3145, 2010

Key words: fracture; FTIR; morphology; structure–property relations

INTRODUCTION

The incorporation of soft rubber particles into the semicrystalline nylon 6 matrix is an effective routine for improving the toughness of such a notch-sensitive engineering plastic with low crack-propagation resistance.[1–6] It is well established that the phase morphology, including particle size and rubber concentration, has a dramatic influence on the toughening efficiency, and several underlying mechanisms have been proposed in past decades. In his pioneering studies, Wu and coworkers[7,8] first suggested that the toughness is controlled by a critical ligament thickness among rubber particles, that is, the surface-to-surface interparticle distance, rather than by the particle size itself, on the basis of the concept of the percolation of overlapped stress fields around rubber particles. Rather, Argon and coworkers[9–11] later argued that the toughening effect stems from the percolation of a preferential crystalline layer with low plastic resistance around rubber particles, which is also related to a critical parameter, that is, interparticle distance. More recently, Corté and Leibler[12] proposed a different model for rubber-toughened semicrystalline polymers based on the two competing processes of matrix shear yielding activated by the rubber particles and brittle fracture caused by the coalescence of microcracks between crystalline lamellae.[12] In their model, similarly, toughness is dominated by a critical distance, which depends not only on the matrix characteristics but also on the particle size.

Despite some controversies in the aforementioned toughening mechanisms, extensive plastic deformation in the matrix without the initiation of any premature fracture processes is crucial for achieving superior toughness in rubber-modified semicrystalline polymers. The role of the dispersed rubber phase is expected to induce an overall plastic deformation in the entire matrix rather than a localized one.[13,14] To date, evidence of plastic deformation at the crack tips has been indirectly deduced from the undulate fracture surface or from the elongated rubber particles embedded in the matrix, mostly by electron microscopy techniques.[9,15,16] The main problem for the *in situ* detection of plastic deformation events at the crack tips arises from the extreme deformation gradient close to the crack tips, which can only be resolved by some specific experimental

Correspondence to: B. Na (bingnash@163.com or bna@ecit.edu.cn).

Contract grant sponsor: National Natural Science Foundation of China; contract grant number: 20704006.
Contract grant sponsor: Natural Science Foundation of Jiangxi, China; contract grant number: 0650009*.
Contract grant sponsor: Project of Jiangxi Provincial Department of Education; contract grant number: GJJ08295.
Contract grant sponsor: Doctor and President Foundation of East China Institute of Technology.

methods with high spatial resolution. In fact, position-resolved X-ray experiments and NMR imaging have been developed to study the structural evolution in the bulk ahead and near the crack tips in poly(vinylidene fluoride),[17] poly(styrene-*co*-acrylonitrile-*co*-butadiene),[18] and rubber-modified nylon 6.[14] In our previous study,[19] alternatively, we demonstrated that spatially resolved micro Fourier transform infrared (micro-FTIR) is powerful for probing the molecular orientation, especially in the amorphous phase at crack tips, which is advantageous over other techniques, such as X-ray scattering measurements.

In this study, we further adopted micro-FTIR measurements to unveil the molecular orientation at the crack tips of rubber-modified nylon 6 with a distinct phase morphology. The results indicate that, at a nearly constant rubber concentration, decreasing the rubber particle size, that is, reducing the interparticle distance indeed promoted the formation of a plastic deformation region at the crack tips, which was manifested by a significant molecular orientation, especially in the amorphous phase. For the first time, a direct correlation was shown between the phase morphology and plastic deformation events at the crack tips; this was beneficial for the further understanding of the toughening mechanism in rubber-modified semicrystalline polymers.

EXPERIMENTAL

Materials and sample preparation

Commercial nylon 6 with an intrinsic viscosity of 1.4 dL/g and ethylene–propylene–diene terpolymer (EPDM; ethylene/propylene/diene = 69/30.5/0.5) with a Mooney viscosity of 20 were obtained from BASF, Germany, and DuPont, USA, respectively. An elastomeric compatibilizer, ethylene–acrylate–maleic anhydride terpolymer (EMH; ethylene/acrylate/maleic anhydride = 68/22/10), was used to tailor the phase morphology of the nylon 6/EPDM blends. Before melt mixing, all of materials were dried in a vacuum oven at 80°C overnight. The components were then melt-blended in an internal mixer at 240°C for 10 min. For comparison, two blends with or without the compatibilizer EMH were prepared: one was a nylon 6/EPDM blend with a weight ratio of 70/30, and the other was a nylon 6/EPDM/EMH blend with a weight ratio of 70/27/3. Films with a thickness of about 80 μ m for the following mechanical tests and micro-FTIR measurements were prepared by the melt compression molding of the as-prepared blends in a hot press at 240°C. After being held in the press for 5 min, the films were quickly transferred to a cold press for rapid cooling to room temperature.

Mechanical tests

Two types of mechanical tests with different sample configurations were performed at room temperature with a universal testing machine (Kaiqiangli Testing Instrument Co., China) with a crosshead speed of 2 mm/min: one was a uniaxial tensile test with dog-bone specimens (4 mm width × 6 mm gauge length), and the other was a deeply double-edge-notched tensile (DDENT) test with precracked specimens with a ligament length of 3 mm. The detailed procedure for the preparation of DDENT specimens can be found elsewhere.[19,20]

Micro-FTIR study

The molecular orientation at crack tips during the stepwise stretching of the DDENT specimen at 2 mm/min was monitored by a Thermo Nicolet infrared microscope (USA) with a mercury–cadmium–tellurium detector coupled with a ministretcher at room temperature. Allowing for the large rubber domain size in the blends without compatibilizer, we used a microsampling area of 40 × 40 μm^2 in this case. After the specimen was stretched to a certain displacement, the transmitted IR light was precisely irradiated on the selected regions at the crack tips of the specimen at loading state by the movement of the sample stage under a charged coupling device (CCD) view system of the IR microscope. At each sampling region, polarized infrared spectra (by rotating a ZnSe polarizer (Thermo Scientific, USA)), parallel and perpendicular to the tensile direction, respectively, were collected with a resolution of 4 cm^{-1}, and a total of 64 scans were added.

Structural characterizations

Scanning electron microscopy

The as-prepared films were first cryogenically broken in liquid nitrogen and then etched in toluene to selectively remove the rubber particles. Morphological observations were conducted on a Hitachi X-650 scanning electron microscope (Japan) operating at an accelerating voltage of 5 kV.

X-ray diffraction

The crystalline phase of as-prepared films was determined by an X-ray diffractometer. The wavelength of the monochromated X-ray was 0.154 nm.

RESULTS AND DISCUSSION

Initial structure

Figure 1 presents the phase morphology of the rubber-modified nylon 6 with and without compatibilizer,

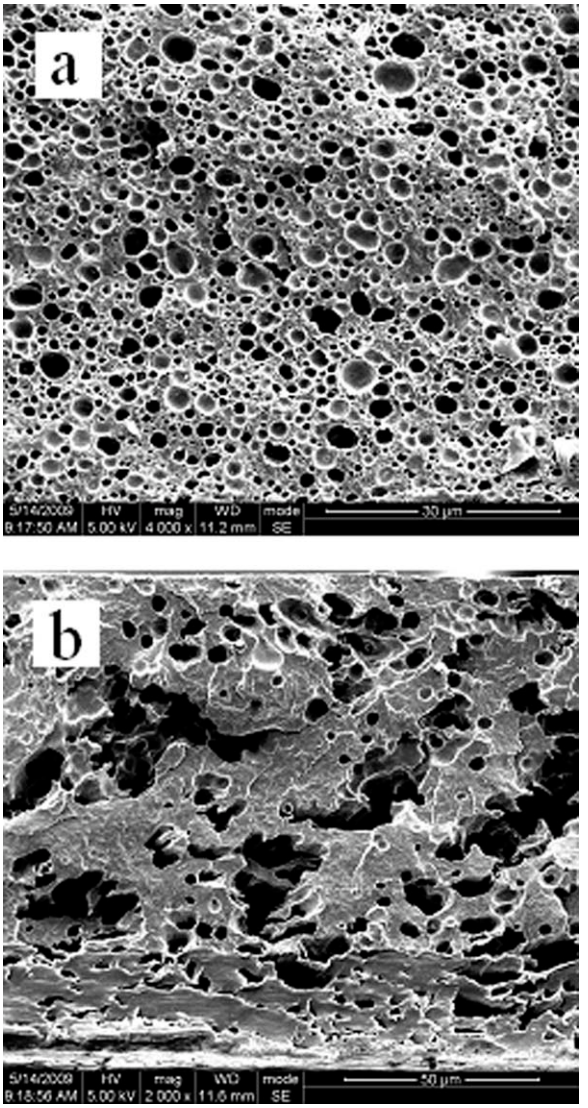

Figure 1 Phase morphology of nylon 6/EPDM blends (a) with and (b) without the compatibilizer. The scale bars correspond to (a) 30 and (b) 50 μm.

respectively. The rubber phase in the blends manifested itself as cavities on the scanning electron microscopy pictures because of selective etching by toluene. The rubber domain size was smaller and more homogeneous in the blends with some amount of EMH, as compared to that without EMH. This strongly indicated that the component EMH acted as a good compatibilizer because of the structural similarity and chemical reaction toward EPDM and nylon 6, respectively.[16,21] The significant compatibilizing effect from EMH reduced the interfacial tension between the dispersed EPDM phase and the nylon 6 matrix during melt mixing and, thus, was responsible for the reduced rubber particles. Moreover, the affinity of EMH toward both EPDM and nylon 6 seemed to be beneficial for the improved mechanical responses in such blends (as presented in the following section). Despite the dramatic change in the phase morphology, the incorporation of the compatibilizer EMH had little influence on the crystalline phase of the nylon 6 matrix, including crystal modification and crystallinity, as shown in Figure 2.

Mechanical responses

Figure 3 shows the mechanical responses of nylon 6/EPDM blends with and without compatibilizer, respectively, with two different types of sample configurations. The results of the uniaxial tensile tests indicate that the incorporation of compatibilizer significantly improved the mechanical properties, including the modulus, yield strength, and elongation at break. This stemmed from the fine dispersion of rubber particles and the enhanced interfacial adhesion between the dispersed EPDM phase and the nylon 6 matrix, as demonstrated previously. Under stretching, a fine and homogeneous dispersion of soft rubber domains redistributed the stress building up around them, and thus, premature fracture due to stress-raising defects could be prevented to a large extent.[12] Furthermore, whereas the interparticle distance was below a critical value, the percolation of overlapped stress fields or of crystalline layers with low plastic resistance around rubber particles could promote the large plastic deformation,[7–11] which could be the situation encountered in the compatibilized nylon 6/EPDM blends with small rubber particles (<1 μm).

On the other hand, compatibilized nylon 6/EPDM blends also exhibited higher stress and elongation during DDENT tests with precracked specimens. The fracture energy, integrated from the profiles of stress versus elongation, was 70.3 versus 29.1 kJ/m^2 for nylon 6/EPDM blends with and without

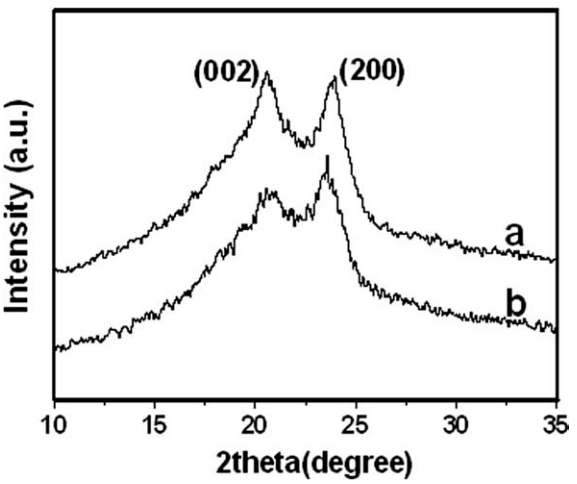

Figure 2 X-ray diffraction profiles obtained from nylon 6/EPDM blends (a) with and (b) without the compatibilizer. The α form, manifested by the characteristic reflections of the (002) and (200) crystal lattices, was present in both blends.

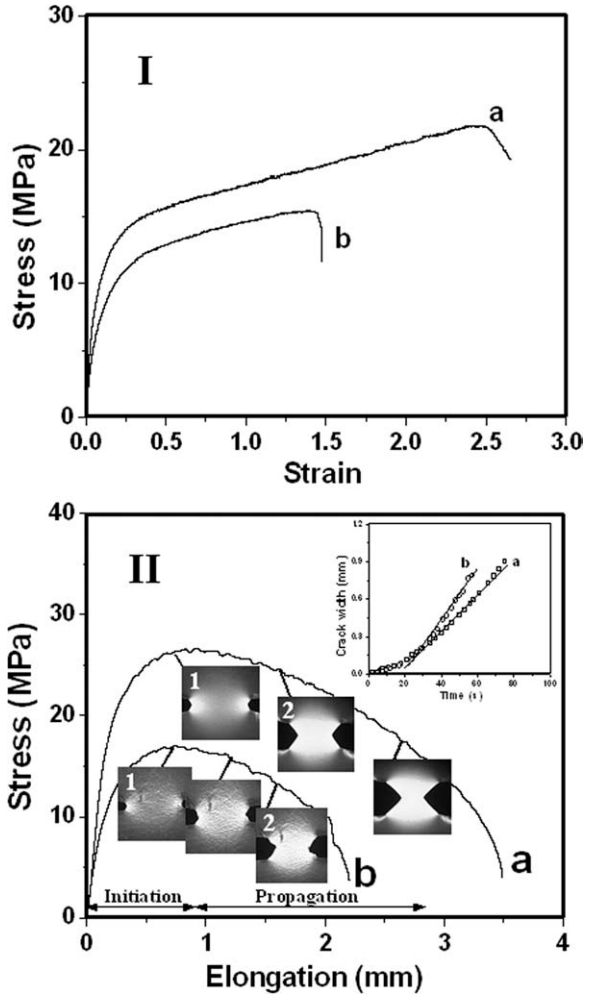

Figure 3 Mechanical responses of nylon 6/EPDM blends (a) with and (b) without the compatibilizer: (I) uniaxial tensile deformation and (II) DDENT deformation. The transverse crack propagation of the samples is included in the inset of part II.

compatibilizer, respectively. With *in situ* registration of the fracture process, moreover, the transverse crack propagation was found to be slower in the compatibilized nylon 6/EPDM blends under the same longitudinal stretching rate, as shown in the inset of Figure 3(II). These results strongly suggest that the incorporation of some amount of EMH component as a compatibilizer significantly enhanced the crack-growth resistance, which found its origin in the reduced rubber domains and improved interfacial adhesion.[1,15]

In addition, accompanied by the formation and growth of the plastic deformation regions around crack tips, stress whitening was observed in both blends, regardless of compatibilizer, as revealed by the simultaneous images monitored by a CCD camera during the fracture process. Macroscopic stress whitening arises from the formation of cavities at a microscopic scale during deformation. However, a close inspection of the images indicated that the cavitation process could be different in two such blends with distinct phase morphologies and interfacial adhesions. According to a pioneering study,[9] it was postulated that the internal cavitation of rubber particles occurred in compatibilized nylon 6/EPDM blends with fine rubber domains and strong interfacial adhesion, whereas cavitation from interfacial debonding could have been responsible for the stress whitening in nylon 6/EPDM blends without compatibilizer. As demonstrated by many researchers,[15,22] it was the internal cavitation of the rubber particles ahead of the cracks in the compatibilized nylon 6/EPDM blends that released the triaxial stresses and, in turn, gave rise to a significant formation of plastic deformation regions and the increased energy dissipation. Even so, as stated in the introduction, the plastic deformation event at the crack tips and its correlation with phase morphology are still poorly understood. Therefore, in the following section, major attention is paid to the exploration of the molecular orientation at the crack tips by micro-FTIR measurements.

Molecular orientation at the crack tips

Like uniaxial stretching, the formation of plastic deformation regions at the crack tips must result in molecular orientation in both the crystalline and amorphous phases. Thus, the order parameters can serve as an indicator to reveal the extent of plastic deformation at the crack tips during the fracture process. Figure 4(a,b) presents the polarized IR spectra, parallel and perpendicular to the stretching direction, respectively, obtained from the small sampling region ahead of the crack tips during the stretching of a DDENT specimen of the compatibilized nylon 6/EPDM blends. In the wave-number range between 1150 and 900 cm^{-1}, two characteristic absorption bands were adopted to characterize the molecular orientation in the nylon 6 matrix during the fracture process:[23,24] one was located at 1122 cm^{-1} and was assigned to the amorphous phase, and the other appeared at 930 cm^{-1} and belonged to the α form of the crystalline phase. The order parameter in both the crystalline and amorphous phases (f)[25] could be deduced as follows:

$$f = (R - 1)/(R + 2) \quad (1)$$

$$R = A_{\parallel}/A_{\perp} \quad (2)$$

where $A_{\parallel}$ and $A_{\perp}$ are the parallel and perpendicular absorbances, respectively.

Figure 5 presents the evolution of order parameter in the crystalline and amorphous phases ahead of the crack tips during the stretching of the DDENT specimens of the nylon 6/EPDM blends with and

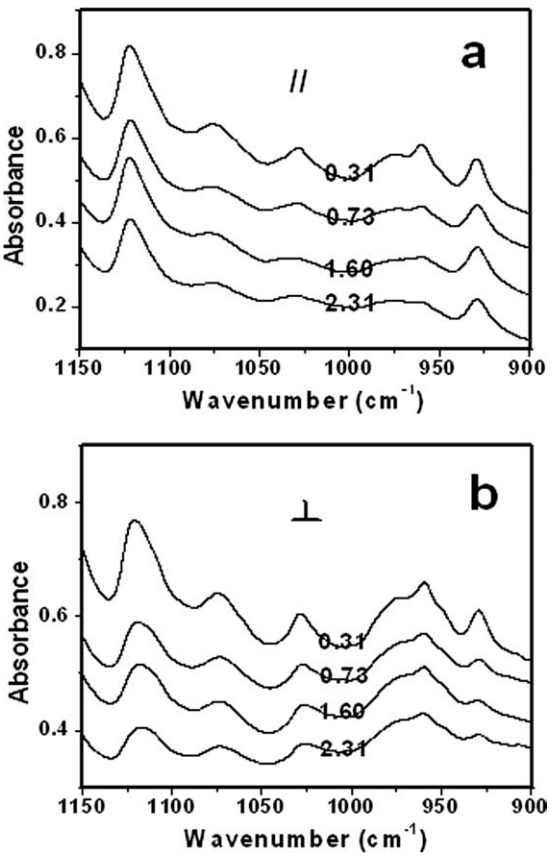

Figure 4 Polarized IR spectra, (a) parallel and (b) perpendicular to the tensile direction, obtained from the small sampling region ahead of the crack tips during the stretching of the nylon 6/EPDM blends with the compatibilizer

without compatibilizer, respectively. In both blends, the molecular orientation of the nylon 6 matrix first increased with elongation and then leveled off, which exactly corresponded to the formation and growth of the plastic deformation region ahead of the crack tips during the fracture process [see Fig. 3(II)]. We expected that, during crack initiation, the molecular chains in both the crystalline and amorphous phase were extended continuously to resist the external force. Once the extension limit of the molecular chains was reached, possibly because of disentanglement, rupture, or pullout from the crystallites,[26] crack propagation occurred subsequently. Herein, the molecular orientation ahead of the crack tips was saturated, and the energy was dissipated to induce the formation and growth of a new plastic region along the transverse direction until ultimate fracture. Higher molecular orientation meant more severe plastic deformation and a higher energy dissipation, which were observed for the compatibilized nylon 6/EPDM blends. Again, this originated from the smaller interparticle distance, which favors the plastic deformation around rubber particles in such compatibilized blends, which is consistent with the prediction of overlapped stress field or the percolation of a preferential crystalline layer with low plastic resistance around the rubber particles. In this study, we could not distinguish which mechanism governed the plastic deformation around the rubber particles according to the molecular orientation determined by the micro-FTIR measurements. However, a direct correlation between the phase morphology and plastic deformation ahead of the crack tips was, indeed, demonstrated experimentally for the first time.

As shown in Figure 5, in addition, the evolution of molecular orientation in the amorphous phase showed a more significant difference between the two blends studied in this case, as compared with that related to the crystalline phase. This means that the segmental extension in the amorphous phase played a more vital role in determining the plastic deformation and fracture process. In fact, numerous studies have demonstrated that the plastic deformation in semicrystalline polymers at large strain is dominated by segmental extension in the amorphous phase rather than by the orientation of crystallites.[27,28]

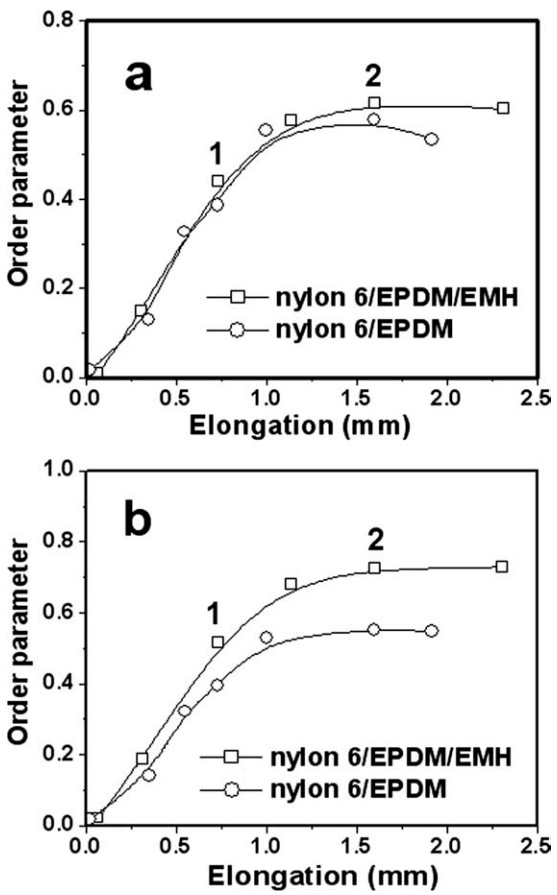

Figure 5 Evolution of the order parameter during the stretching of the DDENT specimens in the small sampling region ahead of the crack tips of the rubber-modified nylon 6: (a) the crystalline phase and (b) the amorphous phase. Numbers 1 and 2 correspond to the numbers presented in Figure 3(II).

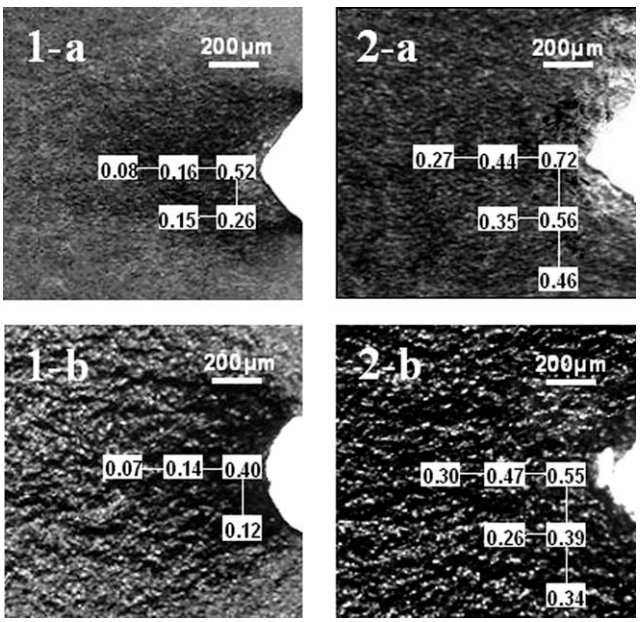

Figure 6 Distribution of the order parameter in the amorphous phase around the crack tips during the stretching of the DDENT specimens of the nylon 6/EPDM blends (a) with and (b) without the compatibilizer to selected elongations. Numbers 1 and 2 correspond to the numbers presented in Figure 3(II).

The rigid crystallites only serve as physical crosslinks for the extension of a flexible molecular network composed by the amorphous phase. This argument seems reasonable for the plastic deformation ahead of the crack tips with significant molecular orientation.

Meanwhile, the tightening of the molecular chains ahead of the crack tips because of orientation can extend the plastic deformation into the adjacent regions parallel and perpendicular to the stretching direction. The formation of a large plastic zone meant significant energy dissipation, which, in turn, gave rise to a high molecular orientation in such damaged regions. To clarify it, the molecular orientation around the crack tips was also measured for the nylon 6/EPDM blends with and without compatibilizer, respectively. Figure 6 presents the distribution of the molecular orientation in the amorphous phase around the crack tips after the DDENT specimens were stretched to two selective elongations, accompanied by the photographs obtained from an optical microscope. Because the molecular orientation in the amorphous phase showed a more significant difference in the two blends than that from the crystalline phase, only the amorphous orientation distribution is presented for comparison. Multiple and homogeneous crazes were formed around the crack tips in the compatibilized nylon 6/EPDM blends as a result of the small interparticle distance and strong interfacial adhesion. Moreover, the plastic damage is suppressed along the transverse direction to a large extent in such compatibilized blends, as compared with that observed in the uncompatibilized nylon 6/EPDM blends with a large rubber domain and weak interfacial adhesion. This means that the incorporation of the compatibilizer EMH significantly enhanced the transverse crack-propagation resistance, and under loading, the plastic deformation extended along the stretching direction easily. Hence, a higher molecular orientation in the regions perpendicular to the crack-propagation direction was expected for the compatibilized nylon 6/EPDM blends, which is shown in Figure 6.

CONCLUSIONS

Experimentally, the molecular orientation at crack tips of rubber modified nylon 6 was explored for the first time by micro-FTIR measurements. It was indicated that there was a strong correlation between the phase morphology and the molecular orientation at the crack tips. At a nearly constant rubber concentration, the decreasing rubber particles promoted molecular orientation, especially in the amorphous phase, as a result of significant plastic deformation induced by the rubber domains, which, in turn, gave rise to dramatic energy dissipation and, thus, superior toughness in the compatibilized nylon 6/EPDM blends. Our results give deep insight into the plastic deformation event at the crack tips, which could be beneficial for the further understanding of the toughening mechanism in rubber-modified semicrystalline polymers.

References

1. Balamurugan, G.; Maiti, S. Polym Test 2008, 27, 752.
2. Oshinski, A.; Keskkula, H.; Paul, D. Polymer 1996, 37, 4891.
3. Oderkerk, J.; Groeninckx, G.; Soliman, M. Macromolecules 2002, 35, 3946.
4. Wang, C.; Su, J.; Li, J.; Yang, H.; Zhang, Q.; Du, R.; Fu, Q. Polymer 2006, 47, 3197.
5. Okada, O.; Keskkula, H.; Paul, D. Polymer 2000, 41, 8061.
6. Modic, M.; Pottick, L. Polym Eng Sci 1993, 33, 819.
7. Wu, S. Polymer 1985, 26, 1855.
8. Margolina, A.; Wu, S. Polymer 1988, 29, 2170.
9. Muratoglu, O.; Argon, A.; Cohen, R.; Weinberg, M. Polymer 1995, 36, 921.
10. Muratoglu, O.; Argon, A.; Cohen, R.; Weinberg, M. Polymer 1995, 36, 4771.
11. Muratoglu, O.; Argon, A.; Cohen, R. Polymer 1995, 36, 2143.
12. Corté, L.; Leibler, L. Macromolecules 2007, 40, 5606.
13. Tzika, P.; Boyce, M.; Parks, D. J Mech Phys Solids 2000, 48, 1893.
14. Adriaensens, P.; Storme, L.; Carleer, R.; D'Haen, J.; Gelan, J.; Litvinov, V.; Marissen, R.; Crevecoeur, J. Macromolecules 2002, 35, 135.
15. Huang, J.; Paul, D. Polymer 2006, 47, 3505.
16. Bhattacharyya, A.; Ghosh, A.; Misra, A.; Eichhorn, K. Polymer 2005, 46, 1661.
17. Maier, G.; Wallner, G.; Lang, R.; Fratzl, P. Macromolecules 2005, 38, 6099.

18. Adriaensens, P.; Storme, L.; Carleer, R.; Vanderzande, D.; Gelan, J.; Litvinov, V.; Marissen, R. Macromolecules 2000, 33, 4836.
19. Xu, W.; Lv, R.; Na, B.; Tian, N.; Li, Z.; Fu, Q. J Phys Chem B 2009, 113, 9664.
20. Na, B.; Lv, R. J Appl Polym Sci 2007, 105, 3274.
21. Carone, E., Jr.; Kopcak, U.; Gonçalves, M.; Nunes, S. Polymer 2000, 41, 5929.
22. Burgisi, G.; Paternoster, M.; Peduto, N.; Saraceno, A. J Appl Polym Sci 1997, 66, 777.
23. Vasanthan, N.; Salem, D. J Polym Sci Part B: Polym Phys 2001, 39, 536.
24. Murthy, N.; Bray, R.; Correale, S.; Moore, R. Polymer 1995, 36, 3863.
25. Siesler, H. Pure Appl Chem 1985, 57, 1603.
26. Thomas, E., Ed. Structure and Properties of Polymers; VCH: Weinheim, 1993.
27. Haward, R. Macromolecules 1993, 26, 5860.
28. Hiss, R.; Hobeika, S.; Lynn, C.; Strobl, G. Macromolecules 1999, 32, 4390.